# Assessing ADI Response Towards Abrasive Wear with Differing Heat Treatment Parameters

Student Names: Daniel Mangeri, Muhammad Ezzam, Zachary Zipf
Faculty Advisors: Prof. Janelle Wharry
Industrial Sponsors: California Pellet Mill

PURDUE UNIVERSITY
School of Materials Engineering

California Pellet Mill (CPM) is aiming to extend the lifetime of grinding and compaction components in their industrial pellet mills used to densify biomass for renewable energy applications. Traditional quench-and-tempered or carburized steels are currently in use, but they exhibit unsatisfactory wear resistance. Austempered ductile iron (ADI) is being considered as an alternative for these high-wear components. This project explores how variations in heat treatment influence the microstructure, mechanical properties, and suitability of ADI for pellet mill components.

This work is sponsored by CPM,1114 E Wabash Ave, Crawfordsville, IN 47933

CALIFORNIA PELLET MILL
Your Partner in Productivity

## Background

***Ductile iron (DI)*** is a form of cast iron containing spherical graphite nodules, which enhance mechanical properties, serve as crack arrestors, and improve toughness and fatigue properties [1].

***Austempering*** is a heat treatment process that entails:

- *Austenitizing* → form an entirely gamma matrix; then
- *Quenching* → to above the martensite start temperature; then
- *Single Step Austempering* → hold at this temperature to nucleate and grow ferrite, which rejects carbon into the austenite making it a metastable phase; OR
- *Dual Step Austempering* → second austempering temperature slightly higher than first step; finer ferrite from first step, second step enhances carbon diffusion to stabilize austenite [2].

Two key microstructural features of ADI are theorized to ***enable greater wear resistance*** [2, 3, 4]:

- *Retained austenite* – Exhibits room temperature strain-induced martensitic phase transformation
- *Plate ferrite* – Finer plate structure improves crack resistance

Higher second step austempering temperature and lower second step austempering times tend to ***increase the volume fraction of retained austenite***, and thus improve wear resistance [2].

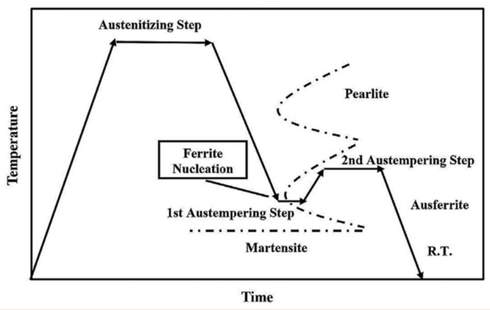


Example of dual-step isothermal heat treatment process [2].

## Experimental Procedures

### Heat Treatment

- Coupon DI samples prepared to ASTM G75 dimension standards
- Wrapped with heat treatment foil to reduce decarburization
- Austenitized in box furnace at 900°C for 2 hours
- Quenched in nitrate salt bath at 250°C for 10 minutes
- Austempering in a second box furnace per experiment matrix
- Four heat treatment parameters had duplicate samples prepared to be sent out for external wear testing. These are designated by a colored box in experiment matrix and are assigned alphabetic nomenclature to be used throughout study

| Austempering Experiment Matrix | | | | |
|---|---|---|---|---|
| Temp (ºC) | Time (min) | | | |
| | 30 | 60 | 90 | 120 |
| 250 | 2 | 1 | 1 | 1 |
| 260 | 1 | 1 | 1 | 1 |
| 280 | 1 | 1 | 1 | 2 |
| 310 | 2 | 1 | 1 | 1 |
| 320 | 1 | 1 | 1 | 1 |
| 340 | - | - | - | 2 |

**Specimen Nomenclature**
A = 250ºC, 30 min
B = 280ºC, 120 min
C = 310ºC, 30 min
D = 340ºC, 120 min

### Slurry Wear Testing

- ASTM G75 slurry wear testing
- Samples A, B, C, D, and a reference quench and tempered DI

### Metallography and Hardness

- Sectioned and mounted in bakelite, polished to 1 µm finish
- Etched with 2% nital for 5-10 seconds
- Rockwell C hardness (5 indents per sample)

### XRD

- PulsTec XRD to obtain integrated intensity of $\alpha_{211}$ and $\gamma_{220}$ peaks
- Calculate retained austenite using ASTM E975-13

### Nanoscratch

- Nanomechanics iMicro with nanoscratch module
- Drag nanoindenter probe of varying load across sample surface
- Array of three scratches performed on samples A, B, C, and D
- Can nanoscratch testing be used as a substitute for ASTM G75?

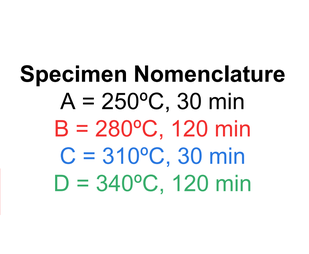


## Results

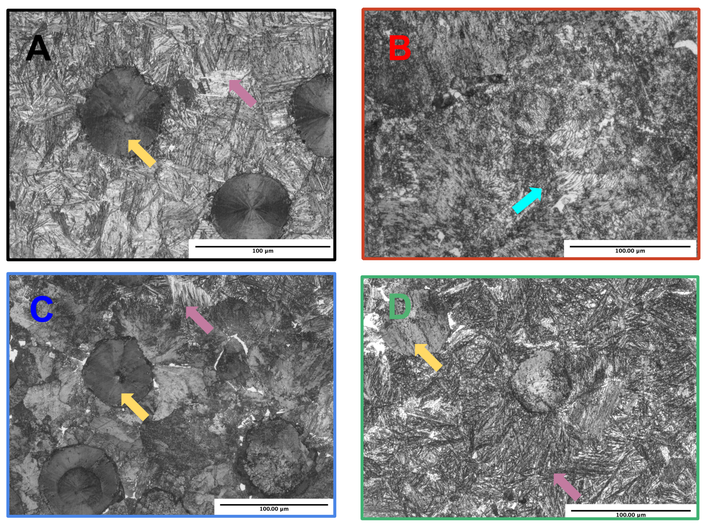


Yellow arrows = spheroidal graphite nodules, purple = ferrite needle, cyan = pearlite

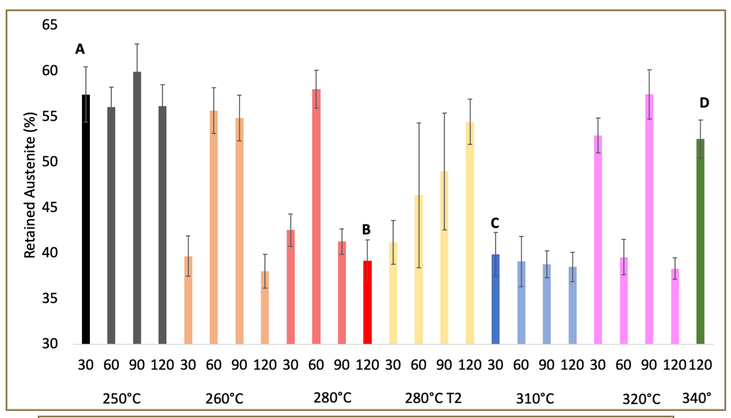


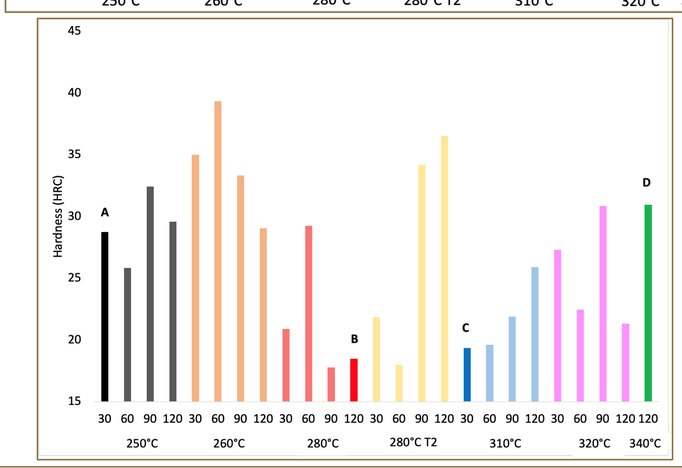


### Nanoscratch

- Records scratch position, load, and surface profile before, during, and after the scratch
- Data was cleaned to zero the surface profile at beginning of scratch (30 µm into the test)

**Top:**
- Profile traces and scratch load as functions of scratch position
- Representative of one scratch on one sample

**Bottom:**
- Average scratch plastic deformation profile (final - initial) as functions of load
- Greater absolute plastic deformation indicates poorer wear resistance
- Deformation energy measured from curve integration

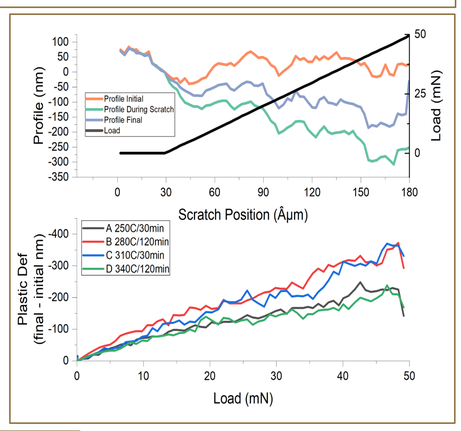


### Slurry Wear Testing

**Right**
- Mass loss (mg) of samples at 2 hour intervals
- Greater mass loss signifies poorer wear resistance

**Bottom**
- Linear and Power function regression parameters

| | P.F. Exponent | P.F. Coefficient | Linear Reg Slope |
|---|---|---|---|
| A | 0.830 | 248 | 181 |
| B | 0.934 | 183 | 163 |
| C | 0.771 | 250 | 164 |
| D | 0.720 | 246 | 147 |

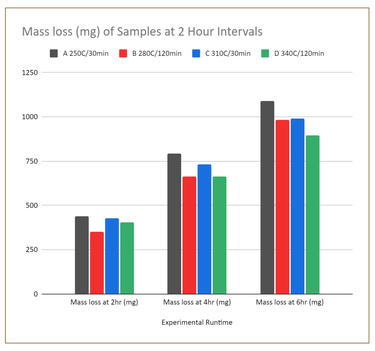


## Discussion

Heat map of regression $R^2$ values between experimental variables. The table is color coded, so that cells with a greener hue have higher correlation ($R^2$ values), and cells with a redder hue have lower correlation.

| | HRC | Vol % RA | Scratch Energy | Scratch Depth |
|---|---|---|---|---|
| Vol % RA | 0.87 | x | x | x |
| Scratch Energy | 0.97 | 0.86 | x | x |
| Scratch Depth | 0.96 | 0.83 | 0.88 | x |
| Mass Loss 2 hr | 0.25 | 0.36 | 0.39 | 0.11 |
| Mass Loss 4 hr | 0.04 | 0.24 | 0.08 | 0.01 |
| Mass Loss 6 hr | 0.01 | 0.07 | 0.00 | 0.02 |
| Slope of Mass Loss | 0.01 | 0.06 | 0.01 | 0.02 |
| Mass Loss Exponent | 0.35 | 0.15 | 0.47 | 0.21 |
| Mass Loss Coeff | 0.33 | 0.31 | 0.49 | 0.17 |

### NanoScratch and Wear Testing

- No strong correlation between nanoscratch and ASTM G75
- Sample A and D have comparable nanoscratch performance
- Sample A and D have opposite G75 performance
- Nanoscratch likely only models surface behavior
- Further investigations might look into nanoscratch performance on electropolished samples

### XRD

- Higher austempering temperature increases the rate of decomposition of austenite
- Quenching process heavily influence the microstructure. Slow quench rate & extended quench time
- T2 heat treatment investigate the influence of quenching rate and time
- Microstructure analysis - 280_120 RA recorded at 39.21% (pearlite). 280_120 T2 recorded 54.44% of RA (ausferrite structure)
- Retained austenite is sacrificed to produce ferrite and high carbon austenite phases (ferrite needles in ausferrite matrix)
- Additional thermal energy gained decomposes high carbon austenite into ferrite & cementite (pearlite)

$$\gamma_o \rightarrow \alpha + \gamma_{HC} \quad (i)$$
$$\gamma_{HC} \rightarrow \alpha + Fe_3C \quad (ii)$$

Phase evolution during austempering [5]

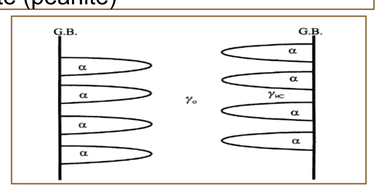


Schematic of ausferrite structure during austempering [5]

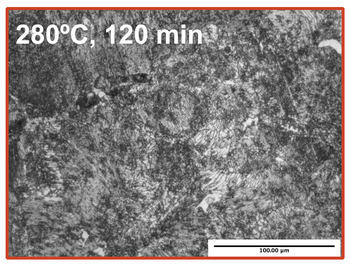


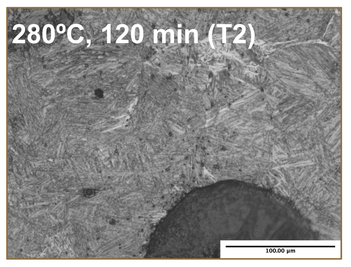


### Microstructure

- Pearlitic structure is abundant in sample 280_120 - should not have formed from the heat treatment parameters
- Quench rate from 900°C to 250°C should have avoided pearlite formation region
- Salt bath was not regulated at target quenching temperature (too high) which reduce quenching rate
- Extended quenching time (30 minutes) - allow decomposition of HC austenite to ferrite & cementite (pearlite)
- T2 iteration – heat treatment strictly follows intended procedures
- 280_120 T2 microstructure mirrored conventional ADI microstructure – does not exhibit pearlitic region

## Conclusions

- Nanoscratch does not sufficiently correlate with G75 to be a substitute
- Further investigation should focus on potential non-linearity of wear behavior
- Quenching time and temperature are a large determinant in microstructural development - transport time between steps and quenching parameters should be closely monitored
- Reasons in difference of wear performance between sample A & D not yet determined, could be related to the presence of blocky ferrite regions and bainite-like microstructure in sample D

**References**

[1] Rio Tinto Iron & Titanium Inc. (1998). *Ductile Iron Data for Design Engineers*.

[2] Wang, B., Barber, G. C., Qiu, F., Zou, Q., & Yang, H. (2020). A review: Phase transformation and wear mechanisms of single-step and dual-step austempered ductile irons. *Journal of Materials Research and Technology*, *9*(1), 1054–1069. https://doi.org/10.1016/j.jmrt.2019.10.074

[3] Sahin, Y., Erdogan, M., & Kilicli, V. (2007). Wear behavior of austempered ductile irons with dual matrix structures. *Materials Science and Engineering: A*, *444*(1-2), 31–38. https://doi.org/10.1016/j.msea.2006.06.071

[4] Hebbar, R. (2011). Investigation on grinding wear behavior of austempered ductile iron as media material during Comminution of iron ore in Ball Mills. *Transactions of the Indian Institute of Metals*, *64*(3), 265–269. https://doi.org/10.1007/s12666-011-0054-0

[5] Janowak, J. F. and Gundlack, R. B., AFS Transactions, 1983,91,377